

# Reactivity of Mo–O<sub>t</sub> Terminal Bonds toward Substrates Having Simultaneous Proton- and Electron-Donor Properties: A Rudimentary Functional Model for Oxotransferase Molybdenum Enzymes<sup>§</sup>

Subodh Kanti Dutta,<sup>†</sup> David B. McConville,<sup>‡</sup> Wiley J. Youngs,<sup>‡</sup> and Muktimoy Chaudhury<sup>\*,†</sup>

Department of Inorganic Chemistry, Indian Association for the Cultivation of Science, Calcutta 700 032, India, and Department of Chemistry, University of Akron, Akron, Ohio 44325-3601

Received June 5, 1996<sup>⊗</sup>

In order to study the reactivity pattern of Mo–O<sub>t</sub> bonds associated with anionic sulfur ligands, precursor complexes MoO<sub>2</sub>L·D (H<sub>2</sub>L = *S*-methyl 3-(2-hydroxyphenyl)methylenedithiocarbamate; D = CH<sub>3</sub>OH (**1**), H<sub>2</sub>O (**2**)) were synthesized. Complex **2** crystallizes in the orthorhombic space group *P*2<sub>1</sub>2<sub>1</sub>2<sub>1</sub>, with *a* = 6.079(1) Å, *b* = 11.638(2) Å, *c* = 17.325(2) Å, *V* = 1225.7(4) Å<sup>3</sup>, and *Z* = 4. In its reaction with PhNHOH, **1** forms a seven-coordinate oxaziridine compound [MoO(η<sup>2</sup>-ONPh)L·CH<sub>3</sub>OH] (**3**) by oxo-rearrangement (elimination–substitution) without a change in the molybdenum oxidation state. The crystal data for **3** are *a* = 9.573(3) Å, *b* = 9.859(2) Å, *c* = 10.604(3) Å, α = 95.90(2)°, β = 95.81(2)°, γ = 112.12(2)°, *V* = 911.5(4) Å<sup>3</sup>, *Z* = 2, and triclinic space group *P*1̄. In contrast to that of the precursor compound **1** (Mo–O<sub>t</sub> = 1.700(4) Å), the terminal Mo–O<sub>t</sub> distance in **3** (1.668(2) Å) is typical of Mo–O bonds of order 3, which drives the formation of an apparently unstable three-membered metallacycle *via* *spectator oxo stabilization* (Rappé, A. K.; Goddard, W. A., III. *J. Am. Chem. Soc.* **1982**, *104*, 448). With thioglycolic acid, **1** undergoes an oxo-transfer reaction through a coupled electron–proton transfer mechanism involving two steps, each having first-order dependence on H<sub>2</sub>tg concentration. The system offers an interesting reactivity model for the oxo-transfer pathway of oxidoreductase Mo enzymes.

## Introduction

The pterin cofactors of oxotransferase molybdenum enzymes have similar minimal structures.<sup>1,2</sup> X-ray crystallographic studies reported recently confirmed that these molecules possess a reduced pyranopterin nucleus with a 6-alkyl side chain carrying an enedithiolate functionality, chelated to a *cis*-MoOX (X = O or S) center.<sup>3,4</sup> Under the constraints of protein microenvironments, reactivity of the Mo–O<sub>t</sub> terminal bond(s) of this *cis*-MoOX moiety appears to be highly interesting.<sup>5</sup> Perhaps a unique combination of size and electronic structure in molybdenum plays a balancing role between the metal ion's abilities to abstract an oxo ligand or to lose it to a substrate, thus catalyzing a host of biological oxo-transfer reactions.<sup>1,6</sup> A mechanistic model proposed for these catalytic actions considers direct transfer of an oxygen atom from the molybdenum center to the substrates<sup>7</sup> (eq 1). This oxo-transfer step is immediately followed by a coupled electron–proton transfer reaction (eq 2)



to reactivate the enzymes. The net process is an oxygen atom transfer reaction involving the elements of water (eq 3) with the molybdenum oxidation state switching between +VI and +IV *via* a short-lived mononuclear EPR-active Mo(V) (*S* = 1/2) intermediate during the turnover.<sup>5a,8,9</sup>

This information has prompted several recent reports on oxomolybdenum complexes of biomimetic ligands.<sup>7d,10–25</sup> Numerous reactions that replicate the primary oxygen atom transfer

<sup>†</sup> Indian Association for the Cultivation of Science.

<sup>‡</sup> University of Akron.

<sup>§</sup> Dedicated to the memory of Professor Nobumasa Kitajima.

<sup>⊗</sup> Abstract published in *Advance ACS Abstracts*, April 15, 1997.

(1) Holm, R. H.; Berg, J. M. *Acc. Chem. Res.* **1986**, *19*, 363.

(2) Rajagopalan, K. V.; Johnson, J. L. *J. Biol. Chem.* **1992**, *267*, 10199 and references therein.

(3) Romao, M. J.; Huber, R. *J. Inorg. Biochem.* **1995**, *59*, 727.

(4) (a) Chan, M. K.; Mukund, S.; Kletzin, A.; Adams, M. W. W.; Rees, D. C. *Science* **1995**, *267*, 1463. (b) Schindelin, H.; Kisker, C.; Hilton, J.; Rajagopalan, K. V.; Rees, D. C. *Science* **1996**, *272*, 1615.

(5) (a) Enemark, J. H.; Young, C. G. *Adv. Inorg. Chem.* **1994**, *40*, 1. (b) *Molybdenum Enzymes, Cofactors and Model Systems*; Stiefel, E. I., Coucouvanis, D., Newton, W. E., Eds.; ACS Symposium Series 535; American Chemical Society: Washington, DC, 1993. (c) Burgmayer, S. J. N.; Stiefel, E. I. *J. Chem. Educ.* **1985**, *62*, 943. (d) *Molybdenum Enzymes*; Spiro, T. G., Ed.; J. Wiley: New York, 1985. (e) *Molybdenum and Molybdenum-Containing Enzymes*; Coughlan, M., Ed.; Pergamon Press: Oxford, England, 1980.

(6) (a) Holm, R. H. *Coord. Chem. Rev.* **1990**, *100*, 183. (b) Holm, R. H. *Chem. Rev.* **1987**, *87*, 1401.

(7) (a) Hille, R.; Sprecher, H. *J. Biol. Chem.* **1987**, *262*, 10914. (b) McWhirter, R. B.; Hille, R. *J. Biol. Chem.* **1991**, *266*, 23724. (c) Schultz, B. E.; Hille, R.; Holm, R. H. *J. Am. Chem. Soc.* **1995**, *117*, 827. (d) Schultz, B. E.; Gheller, S. F.; Muetterties, M. C.; Scott, M. J.; Holm, R. H. *J. Am. Chem. Soc.* **1993**, *115*, 2714. (e) Pietsch, M. A.; Hall, M. B. *Inorg. Chem.* **1996**, *35*, 1273.

(8) Stiefel, E. I. *Proc. Natl. Acad. Sci. U.S.A.* **1973**, *70*, 988.

(9) Bray, R. C. *Q. Rev. Biophys.* **1988**, *21*, 5992.

(10) Fischer, B.; Schmalle, H.; Dubler, E.; Schäfer, A.; Viscontini, M. *Inorg. Chem.* **1995**, *34*, 5726.

(11) Das, S. K.; Chaudhury, P. K.; Biswas, D.; Sarkar, S. *J. Am. Chem. Soc.* **1994**, *116*, 9061.

(12) Pilato, R. S.; Eriksen, K. A.; Greaney, M. A.; Stiefel, E. I.; Goswami, S.; Kilpatrick, L.; Spiro, T. G.; Taylor, E. C.; Rheingold, A. L. *J. Am. Chem. Soc.* **1991**, *113*, 9372.

(13) Eagle, A. A.; Laughlin, L. J.; Youngs, C. G.; Tiekink, E. R. T. *J. Am. Chem. Soc.* **1992**, *114*, 9195.

(14) Dhawan, I. K.; Pacheco, A.; Enemark, J. H. *J. Am. Chem. Soc.* **1994**, *116*, 7911.

(15) Boyde, S.; Ellis, S. R.; Garner, C. D.; Clegg, W. *J. Chem. Soc., Chem. Commun.* **1986**, 1541.

(16) Basu, P.; Raitsimring, A. M.; LaBarre, M. J.; Dhawan, I. K.; Weibrecht, J. L.; Enemark, J. H. *J. Am. Chem. Soc.* **1994**, *116*, 7166.

(17) Peng, G.; Nichols, J.; McCullough, E. A., Jr.; Spence, J. T. *Inorg. Chem.* **1994**, *33*, 2857.

step, both forward and reverse (eq 1), have been achieved with many of these complexes using nitrate, sulfite, benzoin, and a variety of phosphines, amine *N*-oxides, and sulfoxides as substrates. In contrast, examples of model complexes that regenerate *cis*-MoO<sub>2</sub><sup>2+</sup> species *via* a correlated electron–proton transfer step (eq 2) have been few.<sup>26,27</sup>

As part of a program relating to oxo-transfer reactivity of Mo–O<sub>t</sub> terminal bonds toward various electron- and/or proton-donor reagents, we have reported the isolation and characterization of a series of mononuclear molybdenum complexes in biologically relevant oxidation states using derivatives of dithiocarboxylic acids as (S,S)<sup>−</sup> donor ligands.<sup>28–31</sup> Herein we report an extension of this study with a tridentate ligand, *S*-methyl 3-(2-hydroxyphenyl)methylenedithiocarbazate (H<sub>2</sub>L), having (ONS) donor sites. *cis*-MoO<sub>2</sub> complexes of tridentate ligands have a distinct advantage as models for oxo-transfer due to the presence of a labile or vacant coordination site for potential binding of substrates.<sup>32,33</sup> The work presented here includes synthesis of the six-coordinated complexes *cis*-[MoO<sub>2</sub>L·D] (D: CH<sub>3</sub>OH, **1**; H<sub>2</sub>O, **2**) and the crystal structure of **2**. The reactivity of the terminal Mo–O<sub>t</sub> bond toward substrates having simultaneous proton- and electron-donor properties, thioglycolic acid (H<sub>2</sub>tga) and β-phenylhydroxylamine has been investigated.<sup>34,35</sup> Two different kinds of reactivity are observed, oxo-transfer with H<sub>2</sub>tga and oxo-rearrangement (elimination–substitution) with PhNH<sub>2</sub>OH. In the latter case, the product has been identified by X-ray crystallographic analysis. The kinetics of the oxo-transfer reaction with H<sub>2</sub>tga have been investigated in detail.

During the progress of this work, Bhattacharyya *et al.*<sup>36</sup> reported the synthesis and characterization of similar *cis*-MoO<sub>2</sub><sup>2+</sup> complexes of H<sub>2</sub>L and related ligands.

## Experimental Section

All operations were carried out under purified dinitrogen. Reagent grade solvents, dried and distilled by standard methods,<sup>37</sup> were used in all cases unless otherwise mentioned. [MoO<sub>2</sub>(acac)<sub>2</sub>]<sup>38</sup> (Hacac =

acetylacetonone), *S*-methyl dithiocarbazate,<sup>39</sup> β-phenylhydroxylamine,<sup>40</sup> and H<sub>2</sub>L<sup>41</sup> were prepared as previously described. Carbon disulfide, hydrazine hydrate (both from E. Merck), methyl iodide (Loba), acetylacetonone (Fluka), and salicylaldehyde (BDH) were freshly distilled before use. All other chemicals were obtained commercially and used as received.

**Syntheses. [MoO<sub>2</sub>L·CH<sub>3</sub>OH], **1**.** A methanolic solution (30 mL) of [MoO<sub>2</sub>(acac)<sub>2</sub>] (0.65 g, 2 mmol) was added to a suspension of the ligand (H<sub>2</sub>L) in an equimolar amount (0.45 g) in the same solvent (30 mL). The mixture was stirred for 2 h, resulting in a clear orange solution. The volume of the solution was concentrated to *ca.* 10 mL, after which orange crystals appeared during slow cooling in the air. The solid was filtered off, washed with diethyl ether, and finally dried under vacuum. The product was recrystallized from methanol. Yield: 0.69 g (90%). Anal. Calcd for MoC<sub>10</sub>H<sub>12</sub>N<sub>2</sub>O<sub>4</sub>S<sub>2</sub>: C, 31.25; H, 3.12; N, 7.29; Mo, 25.0. Found: C, 31.4; H, 3.2; N, 7.3; Mo, 24.8. IR (KBr pellet), cm<sup>−1</sup>: ν(C<sup>−</sup>N) 1590 s; ν(C–O/phenolate) 1540 s; ν(Mo=O) 930 s, 900 s; ν(C–S) 642 m. UV–vis (CH<sub>3</sub>OH) [λ<sub>max</sub>/nm (ε/M<sup>−1</sup> cm<sup>−1</sup>): 405 (3070), 344 (26 400), 317 (31 200).

**[MoO<sub>2</sub>L·H<sub>2</sub>O], **2**.** This compound was prepared by following the same procedure as described for **1** using wet ethanol as solvent. It was recrystallized from absolute ethanol. Yield: 88%. Anal. Calcd for MoC<sub>9</sub>H<sub>10</sub>N<sub>2</sub>O<sub>4</sub>S<sub>2</sub>: C, 29.19; H, 2.70; N, 7.56; Mo, 25.95. Found: C, 29.1; H, 2.6; N, 7.5; Mo, 25.5. IR (KBr pellet), cm<sup>−1</sup>: ν(OH) 3320 b; ν(C<sup>−</sup>N) 1590 s; ν(C–O/phenolate) 1545 s; ν(Mo=O) 940 s, 910 s; ν(C–S) 642 m. UV–vis (CH<sub>3</sub>OH) [λ<sub>max</sub>/nm (ε/M<sup>−1</sup> cm<sup>−1</sup>): 402 (3000), 340 (25 300), 310 (32 000).

Diffraction-quality crystals were grown from absolute ethanol by slow evaporation.

**[MoO(η<sup>2</sup>-ONPh)L·CH<sub>3</sub>OH], **3**.** To a stirred suspension of **1** (0.55 g, 1.45 mmol) in methanol (60 mL) was added a solid sample of β-phenylhydroxylamine (0.17 g, 1.55 mmol) in portions. A darker clear solution was obtained which was reduced to *ca.* 20 mL in volume on a rotary evaporator. On standing at room temperature, the solution yielded shining brown crystals. These were collected by filtration, washed with Et<sub>2</sub>O, and dried under vacuum. Yield: 0.55 g (80%). Anal. Calcd for MoC<sub>16</sub>H<sub>17</sub>N<sub>3</sub>O<sub>4</sub>S<sub>2</sub>: C, 40.42; H, 3.57; N, 8.84; Mo, 20.21. Found: C, 40.3; H, 3.6; N, 8.9; Mo, 20.2. IR (KBr pellet), cm<sup>−1</sup>: ν(C<sup>−</sup>N) 1590 s; ν(C–O/phenolate) 1540 s; ν(Mo=O) 975 s; ν(C–S) 640 m. UV–vis (CH<sub>3</sub>OH) [λ<sub>max</sub>/nm (ε/M<sup>−1</sup> cm<sup>−1</sup>): 433 (sh), 362 (10 900), 322 (18 200).

Diffraction-quality crystals were obtained from methanol by slow evaporation.

**[MoOL], **4**. Method 1.** To a stirred suspension of **1** (0.19 g, 0.5 mmol) in CH<sub>3</sub>OH (30 mL) was added a solution of thioglycolic acid (H<sub>2</sub>tga) (0.1 g, *ca.* 1 mmol) in the same solvent (5 mL). Stirring was continued for 2 h at room temperature, during which the color of the reaction mixture changed to dark-brown from its initial orange shade. It was filtered and the filtrate volume reduced to *ca.* 15 mL by rotary evaporation. The dark microcrystalline compound obtained at this stage was collected by filtration, washed with Et<sub>2</sub>O, and dried under vacuum. Recrystallization was not possible due to the low solubility of this compound in common organic solvents. Yield: 0.11 g (65%).

**Method 2.** A mixture of **1** (0.27 g, 0.7 mmol) and PPh<sub>3</sub> (0.37 g, 1.4 mmol) in methanol (40 mL) was refluxed for 2 h, during which a dark, shining microcrystalline product appeared. It was collected by filtration, washed with Et<sub>2</sub>O, and dried under vacuum. Yield: 0.18 g (76%). Anal. Calcd for MoC<sub>9</sub>H<sub>8</sub>N<sub>2</sub>O<sub>2</sub>S<sub>2</sub>: C, 32.14; H, 2.38; N, 8.33; Mo, 28.57. Found: C, 31.8; H, 2.3; N, 8.1; Mo, 28.2. IR (KBr pellet), cm<sup>−1</sup>: ν(C<sup>−</sup>N) 1590 s; ν(C–O/phenolate) 1530 s; ν(Mo=O) 962 s; ν(C–S) 630 m. UV–vis (DMF) [λ<sub>max</sub>/nm (ε/M<sup>−1</sup> cm<sup>−1</sup>): 680 (sh), 471 (5600), 402 (sh), 365 (sh), 309 (11 800).

**Physical Measurements.** Details of IR and UV–visible measurements have been described elsewhere.<sup>42</sup> Elemental analyses for C, H, and N were performed in this laboratory (IACS) with a Perkin-Elmer

- (18) Oku, H.; Ueyama, N.; Kondo, M.; Nakamura, A. *Inorg. Chem.* **1994**, *33*, 209.
- (19) Roberts, S. A.; Young, C. G.; Cleland, W. E., Jr.; Ortega, R. B.; Enemark, J. H. *Inorg. Chem.* **1988**, *27*, 3044.
- (20) Harlan, E. W.; Berg, J. M.; Holm, R. H. *J. Am. Chem. Soc.* **1986**, *108*, 6992.
- (21) Gheller, S. F.; Schultz, B. E.; Scott, M. J.; Holm, R. H. *J. Am. Chem. Soc.* **1992**, *114*, 6934.
- (22) Roberts, S. A.; Young, C. G.; Kipke, C. A.; Cleland, W. E., Jr.; Yamanouchi, K.; Carducci, M. D.; Enemark, J. H. *Inorg. Chem.* **1990**, *29*, 3650.
- (23) Craig, J. A.; Holm, R. H. *J. Am. Chem. Soc.* **1989**, *111*, 2111.
- (24) Ueyama, N.; Yoshinaga, N.; Nakamura, A. *J. Chem. Soc., Dalton Trans.* **1990**, 387.
- (25) Berg, J. M.; Holm, R. H. *J. Am. Chem. Soc.* **1985**, *107*, 917.
- (26) Xiao, Z.; Youngs, C. G.; Enemark, J. H.; Wedd, A. G. *J. Am. Chem. Soc.* **1992**, *114*, 9194.
- (27) Young, C. G.; Wedd, A. G. In *Encyclopedia of Inorganic Chemistry*; King, R. B., Ed.; Wiley: New York, 1994; p 2330 and references therein.
- (28) Dutta, S. K.; Kumar, S. B.; Bhattacharyya, S.; Chaudhury, M. *J. Chem. Soc., Dalton Trans.* **1994**, 97.
- (29) Kumar, S. B.; Chaudhury, M. *J. Chem. Soc., Dalton Trans.* **1990**, 2169.
- (30) Chaudhury, M. *Inorg. Chem.* **1985**, *24*, 3011.
- (31) Chaudhury, M. *Inorg. Chem.* **1984**, *23*, 4434.
- (32) Topich, J.; Lyon, J. T., III. *Inorg. Chem.* **1984**, *23*, 3202.
- (33) Craig, J. A.; Harlan, E. W.; Snyder, B. S.; Whitener, M. A.; Holm, R. H. *Inorg. Chem.* **1989**, *28*, 2082.
- (34) Martin, J. F.; Spence, J. T. *J. Phys. Chem.* **1970**, *74*, 3589.
- (35) Thakuria, B. M.; Gupta, Y. K. *J. Chem. Soc., Dalton Trans.* **1975**, 77.
- (36) Bhattacharjee, S.; Bhattacharyya, R. *J. Chem. Soc., Dalton Trans.* **1993**, 1151.
- (37) Perrin, D. D.; Armarego, W. L. F.; Perrin, D. R. *Purification of Laboratory Chemicals*, 2nd ed.; Pergamon: Oxford, England, 1980.

- (38) Chen, G. J.-J.; McDonald, J. W.; Newton, W. E. *Inorg. Chem.* **1976**, *15*, 2612.

- (39) Bohr, G.; Sehleitzer, G. Z. *Anorg. Allg. Chem.* **1955**, *280*, 176.

- (40) Vogel, A. I. *A Text-Book of Practical Organic Chemistry*, 3rd ed.; Longman: London, 1973; p 629.

- (41) Dutta, S. K.; Tiekink, E. R. T.; Chaudhury, M. *Polyhedron*, in press.

**Table 1.** Summary of Crystallographic Data

	2	3
formula	C <sub>9</sub> H <sub>10</sub> N <sub>2</sub> O <sub>4</sub> S <sub>2</sub> Mo	C <sub>16</sub> H <sub>17</sub> N <sub>3</sub> O <sub>4</sub> S <sub>2</sub> Mo
fw	370.25	475.38
space group	P2 <sub>1</sub> 2 <sub>1</sub> 2 <sub>1</sub> (No. 19)	P1̄ (No. 2)
a, Å	6.079(1)	9.573(3)
b, Å	11.638(2)	9.859(2)
c, Å	17.325(2)	10.604(3)
α, deg		95.90(2)
β, deg		95.81(2)
γ, deg		112.12(2)
V, Å <sup>3</sup>	1225.7(4)	911.5(4)
Z	4	2
T, K	140	140
λ(Mo Kα), Å	0.710 73	0.710 73
ρ <sub>calcd</sub> , g cm <sup>-3</sup>	2.006	1.728
μ, cm <sup>-1</sup>	14.17	9.76
no. of params refined	171	236
R1 <sup>a</sup> (wR2 <sup>b</sup> )	0.0143 (0.0371)	0.0257 (0.0641)

<sup>a</sup> R1 =  $\sum ||F_o| - |F_c|| / \sum |F_o|$ . <sup>b</sup> wR2 =  $[\sum (w(F_o^2 - F_c^2)^2) / \sum (w(F_o^2)^2)]^{1/2}$ .  $w = 1/[\sigma^2(F_o^2) + (dP)^2 + eP]$ , where  $P = (F_o^2 + 2F_c^2)/3$ ,  $d = 0.0279$  and  $e = 0.0000$  for **2**, and  $d = 0.0326$  and  $e = 1.0823$  for **3**.

2400 elemental analyzer. Molybdenum content was estimated gravimetrically as the quinolin-8-olate.

**X-ray Crystallography.** The X-ray data collection on crystals of **2** and **3**, both orange blocks of dimensions (0.40 × 0.30 × 0.18) and (0.36 × 0.22 × 0.18 mm), respectively, was performed on a Syntex P2<sub>1</sub> diffractometer equipped with graphite-monochromated Mo Kα (λ = 0.710 73 Å) radiation. Automatic centering and least-squares routines were carried out on several reflections between 20 and 30° in 2θ (31 for complex **2** and 26 for complex **3**) to obtain the cell dimensions. The intensity data were collected at 140 K using the ω-scan method in the range 4.2 ≤ 2θ ≤ 46.36° for **2**; the corresponding range for **3** was 3.9 ≤ 2θ ≤ 47.82°. For compound **2**, a total of 1444 (3409 for **3**) reflections were scanned, and of these, 1322 (2833 for **3**) independent reflections were used for structure solution and refinement. Three standard reflections measured every 97 reflections showed no significant fluctuation in intensity. The data were corrected for Lorentz and polarization effects. A semiempirical absorption correction (transmission factors were in the ranges 0.624–0.731 for **2** and 0.762–0.846 for **3**) from ψ scans was applied.

The structure of **2** was solved using the automated Patterson routine in the SHELXTL PLUS package,<sup>43</sup> while the structure of **3** was solved by the direct methods program SIR 92.<sup>44</sup> Both structures were refined using SHELXL-93<sup>45</sup> via full-matrix least-squares calculations on F<sup>2</sup>. All non-hydrogen atoms were refined with anisotropic thermal parameters, and hydrogen atoms were placed in calculated positions and refined using a riding model. Refinement to convergence of 171 parameters against all 1322 unique data yielded wR2 = 3.71%, GOF = 1.054 (R1 = 1.43% for I > 2.0σ(I)) for complex **2**. For complex **3**, 236 parameters were refined using all 2833 unique data to give wR2 = 6.41%, GOF = 1.038 (R1 = 2.57% for I > 2.0σ(I)). Conventional R factors, R1, are based on F while weighted R factors, wR2, are based on F<sup>2</sup>. Relevant crystallographic data and the details of final refinement processes are provided in Table 1.

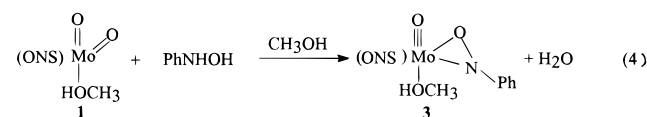
**Kinetics Measurements.** All manipulations associated with the kinetic measurements were performed under a dinitrogen atmosphere. Approximately 10<sup>-4</sup> M solutions of **1** in dry methanol were employed. For each molybdenum concentration, experiments were carried out with five or more different H<sub>2</sub>tga concentrations and the kinetics followed for at least 3 half-lives. Pseudo-first-order conditions were used throughout by maintaining the H<sub>2</sub>tga concentration between 20- and 60-fold molar excess over the molybdenum concentration. Each

experiment was repeated at least three times, and the solutions were maintained at a constant temperature (±0.1 °C) with a Haake F3 thermostated bath. Absorption changes at 425 nm during the course of reaction were monitored by conventional spectrophotometry using a Shimadzu UV-2100 spectrophotometer. All computation work for the analyses of kinetic data were performed on an IBM PC 486 computer using a locally developed least-squares program.

## Results and Discussion

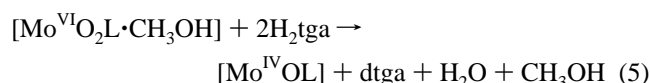
**Synthesis.** The orange complex [Mo<sup>VI</sup>O<sub>2</sub>L·CH<sub>3</sub>OH], **1**, is obtained by the reaction of [MoO<sub>2</sub>(acac)<sub>2</sub>] with a stoichiometric amount of H<sub>2</sub>L in methanol at room temperature. When wet ethyl alcohol is used as solvent, the corresponding product is [Mo<sup>VI</sup>O<sub>2</sub>L·H<sub>2</sub>O], **2**. Both these complexes are soluble in common organic solvents. In the solid state, **1** loses the coordinated methanol slowly with simultaneous disappearance of its shining nature. The product is probably an oxo-bridged oligomer,<sup>46</sup> revertible to its original mononuclear form when recombined with dry methanol.

Reaction of **1** with β-phenylhydroxylamine in methanol (eq 4) involves an oxo-rearrangement process. The Mo(VI) product



**3**, which is stable at room temperature, has two interesting features. It contains a three-membered molybdoxaziridine<sup>47</sup> (MoON) ring. The remaining Mo–O<sub>t</sub> bond (spectator) appears to be converted from a double to a triple bond, as suggested by X-ray crystallographic analysis (*vide infra*). Thus the seemingly innocent spectator oxo group may be intimately involved in stabilization of the three-membered metallacycle. This experimental observation is in complete agreement with the predictions of Rappé and Goddard from *ab initio* theoretical calculations.<sup>48</sup> Compound **3** is soluble in methanol and CH<sub>2</sub>Cl<sub>2</sub>.

Treatment of **1** with H<sub>2</sub>tga (1:2 mole ratio) generates the monooxo Mo(IV) complex [MoOL], **4**, and dtga, the oxidized form of thioglycolic acid<sup>34</sup> by an oxo-abstraction reaction, shown by eq 5. The kinetics and mechanism of this reaction have been



examined in detail (*vide infra*). Compound **4**, once isolated, fails to react with Lewis bases such as pyridine, picoline, or imidazole, suggesting a polymeric structure, perhaps binuclear.<sup>49</sup> This dark-brown Mo(IV) compound can also be prepared by an alternative route (method 2) using PPh<sub>3</sub> as the oxo abstractant. It is sparingly soluble in common organic solvents except in DMF in which it has only limited stability, thus eluding all attempts at recrystallization.

The free ligand H<sub>2</sub>L exhibits a ν(C=S) vibration at 1040 cm<sup>-1</sup>, as well as ν(N–H) at ca. 2960 and ν(O–H) at 3100 cm<sup>-1</sup>. All of these suggest that the Schiff base ligand is in its thione form.<sup>36</sup> The disappearance of these bands and appearance of a new band at 645–630 cm<sup>-1</sup> due to the ν(C–S) stretch indicate a tridentate ONS mode of coordination from the thioenol<sup>36</sup> form in the complexes. Compounds **1** and **2** both show two strong

(42) Bhattacharyya, S.; Kumar, S. B.; Dutta, S. K.; Tiekink, E. R. T.; Chaudhury, M. *Inorg. Chem.* **1996**, *35*, 1967.

(43) SHELXTL PLUS; Siemens Analytical X-ray Instruments, Inc.: Madison, WI, 1994.

(44) Altomare, A.; Cascarano, G.; Giacovazzo, C.; Guagliardi, A.; Burla, M. C.; Polidori, G.; Camalli, M. *J. Appl. Crystallogr.* **1994**, *27*, 435.

(45) Sheldrick, G. M. SHELXL-93: Program for the Refinement of Crystal Structures. University of Göttingen, Germany, 1993.

(46) Rajan, O. A.; Chakravorty, A. *Inorg. Chem.* **1981**, *20*, 660.

(47) Liebeskind, L. S.; Sharpless, K. B.; Wilson, R. D.; Ibers, J. A. *J. Am. Chem. Soc.* **1978**, *100*, 7061.

(48) Rappé, A. K.; Goddard, W. A., III. *J. Am. Chem. Soc.* **1982**, *104*, 448.

(49) Caradonna, J. P.; Harlan, E. W.; Holm, R. H. *J. Am. Chem. Soc.* **1986**, *108*, 7856.

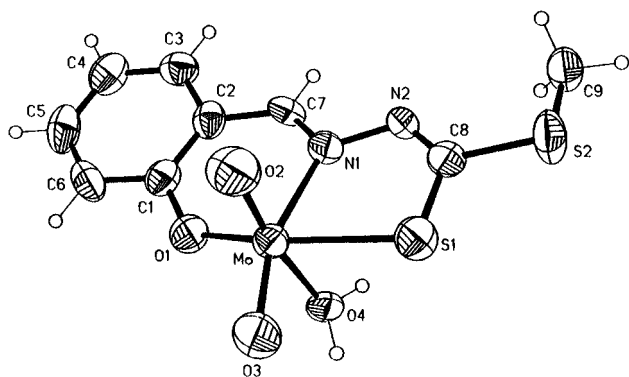


**Figure 1.** Molecular structure and crystallographic numbering scheme for the complex  $[\text{MoO}_2\cdot\text{L}\cdot\text{H}_2\text{O}]_2$ , **2**.

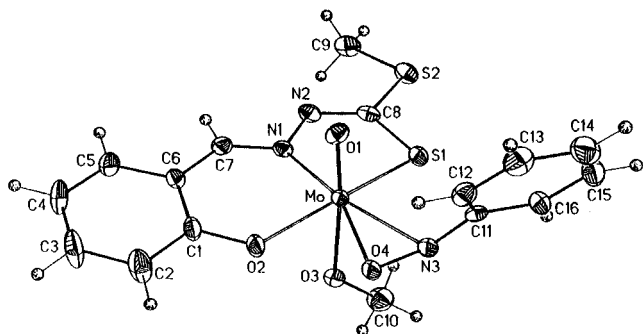


**Figure 2.** Molecular structure and crystallographic numbering scheme for the complex  $[\text{MoO}(\text{ONPh})\cdot\text{L}\cdot\text{CH}_3\text{OH}]$ , **3**.

**Table 2.** Selected Bond Distances and Angles for **2**

Distances (Å)			
Mo–O(3)	1.697(2)	S(1)–C(8)	1.740(3)
Mo–O(2)	1.702(2)	S(2)–C(8)	1.739(3)
Mo–O(1)	1.928(2)	O(1)–C(1)	1.344(4)
Mo–N(1)	2.275(3)	N(1)–C(7)	1.286(4)
Mo–O(4)	2.308(2)	N(1)–N(2)	1.406(4)
Mo–S(1)	2.4403(9)	N(2)–C(8)	1.291(4)
Angles (deg)			
O(3)–Mo–O(2)	105.9(1)	O(3)–Mo–S(1)	91.12(7)
O(3)–Mo–O(1)	104.04(9)	O(2)–Mo–S(1)	97.01(8)
O(2)–Mo–O(1)	99.3(1)	O(1)–Mo–S(1)	153.65(7)
O(3)–Mo–N(1)	158.81(9)	N(1)–Mo–S(1)	75.86(7)
O(2)–Mo–N(1)	92.4(1)	O(4)–Mo–S(1)	80.79(6)
O(1)–Mo–N(1)	82.88(9)	C(8)–S(1)–Mo	100.5(1)
O(3)–Mo–O(4)	84.27(9)	C(1)–O(1)–Mo	133.6(2)
O(2)–Mo–O(4)	169.69(9)	C(7)–N(1)–Mo	123.6(2)
O(1)–Mo–O(4)	79.46(8)	N(2)–N(1)–Mo	122.8(2)
N(1)–Mo–O(4)	77.26(9)	N(2)–C(8)–S(1)	126.7(2)

bands at *ca.* 930 and 900  $\text{cm}^{-1}$ , assigned to symmetric and antisymmetric vibrations, respectively, of the *cis*- $\text{MoO}_2$  core. As expected, compounds **3** and **4** each show only one such terminal  $\nu(\text{Mo}=\text{O})$  absorption at 975 and 962  $\text{cm}^{-1}$ , respectively.

**Description of the Crystal Structures.** The molecular structures and the atom-numbering schemes for compounds **2** and **3** are shown in Figures 1 and 2, respectively. Selected bond lengths and angles are given in Tables 2 and 3. Complex **2** has a distorted octahedral geometry (Figure 1) with one nitrogen, one sulfur, and four oxygen atoms. Three atoms, O(1), N(1), and S(1) (from the tridentate ligand), and one terminal oxo atom, O(3), occupy the meridional plane and lie  $-0.092(1)$ ,  $-0.028(1)$ ,  $-0.065(1)$ , and  $-0.071(1)$  Å, respectively, out of the least-squares plane through them; the Mo atom lies  $0.256(1)$  Å out of this plane in the direction of the O(2) atom, the other terminal oxygen. Both O(2) and O(4), the latter from the coordinated water molecule, occupy the axial positions and form an O(2)–

**Table 3.** Selected Bond Distances and Angles for **3**

Distances (Å)			
Mo–O(4)	1.965(2)	S(1)–C(8)	1.739(3)
Mo–O(2)	2.006(2)	S(2)–C(8)	1.743(3)
Mo–N(3)	2.091(2)	O(2)–C(1)	1.330(4)
Mo–O(1)	1.668(2)	O(4)–N(3)	1.386(3)
Mo–N(1)	2.180(2)	N(1)–C(7)	1.298(4)
Mo–O(3)	2.321(2)	N(1)–N(2)	1.417(3)
Mo–S(1)	2.417(1)	N(3)–C(11)	1.442(4)
Angles (deg)			
O(1)–Mo–O(4)	100.5(1)	O(4)–Mo–S(1)	115.89(7)
O(1)–Mo–O(2)	102.4(1)	O(2)–Mo–S(1)	153.01(7)
O(4)–Mo–O(2)	78.07(9)	N(3)–Mo–S(1)	76.24(7)
O(1)–Mo–N(3)	103.3(1)	N(1)–Mo–S(1)	77.53(7)
O(4)–Mo–N(3)	39.81(9)	O(3)–Mo–S(1)	83.79(6)
O(2)–Mo–N(3)	115.71(9)	C(8)–S(1)–Mo	98.7(1)
O(1)–Mo–N(1)	92.12(9)	C(1)–O(2)–Mo	132.1(2)
O(4)–Mo–N(1)	159.75(9)	C(10)–O(3)–Mo	130.5(2)
O(2)–Mo–N(1)	83.81(9)	N(3)–O(4)–Mo	75.0(1)
N(3)–Mo–N(1)	151.0(1)	C(7)–N(1)–Mo	125.3(2)
O(1)–Mo–O(3)	174.24(9)	N(2)–N(1)–Mo	123.1(2)
O(4)–Mo–O(3)	83.80(8)	O(4)–N(3)–C(11)	112.0(2)
O(2)–Mo–O(3)	74.57(9)	O(4)–N(3)–Mo	65.2(1)
N(3)–Mo–O(3)	82.42(9)	C(11)–N(3)–Mo	117.2(2)
N(1)–Mo–O(3)	82.72(8)	C(12)–C(11)–N(3)	123.7(3)
O(1)–Mo–S(1)	97.66(8)	C(16)–C(11)–N(3)	116.3(3)

Mo–O(4) angle of  $169.69(9)^\circ$ . Thus the  $\text{MoO}_2$  moiety has a *cis* configuration with conventional<sup>50</sup> average values for the Mo–O(2)/O(3) distance (1.70 Å) and O(2)–Mo–O(3) bond angle ( $105.9(1)^\circ$ ), which is close to the energy-minimum value estimated from MO theory.<sup>51</sup> The Mo–O(4) bond *trans* to the terminal oxygen atom O(2) has been significantly lengthened (2.308(2) Å) compared to the Mo–O(1) distance (1.928(2) Å) occupying a *cis* position, indicating that the  $\text{H}_2\text{O}$  molecule is weakly coordinated to the metal center.

The molecular structure of **3** confirms seven-coordination with an  $\eta^2$ -disposition of the ONPh group around molybdenum. The  $\text{MoO}_4\text{N}_2\text{S}$  core defines a distorted pentagonal-bipyramidal geometry with the planar ONS donor ligand displaying *mer* coordination along with the O(4) and N(3) atoms of the ONPh group (Figure 2). Such a coordination geometry is a common feature for seven-coordinate monooxomolybdenum(VI) complexes.<sup>47,52–54</sup> In this description, the terminal oxo ligand O(1) occupies one of the axial positions, the other being occupied by an oxygen atom, O(3), of a coordinated methanol molecule. N(3), O(4), O(2), N(1), and S(1) define the pentagonal plane about the Mo atom and lie  $-0.031(2)$ ,  $0.105(2)$ ,  $-0.106(1)$ ,  $0.085(1)$ , and  $-0.053(1)$  Å, respectively, out of the weighted least-squares plane through them. The Mo atom is  $0.323(1)$  Å above this plane in the direction of the O(1) atom. Replacement of a strongly  $\pi$ -donating terminal oxo ligand in **2** by the  $\eta^2$ -ONPh moiety drastically reduces the bond length between Mo and the spectator oxygen O(1) in **3** from 1.700(4) to 1.668(2) Å. The latter is typical of Mo–O bonds of order 3.<sup>55</sup> The Mo–O(3) axial bond (2.321(2) Å) is much longer, indicating the strong *trans*-labilizing influence of the Mo–O(1) terminal bond. The Mo–N(1) distance (2.180(2) Å) in **3**, on the other hand, is shortened compared to the corresponding distance (2.275(3) Å) in the parent compound **2**, another effect of this oxo-rearrange-

(50) Ueyama, N.; Oku, H.; Kondo, M.; Okamura, T.; Yoshinaga, N.; Nakamura, A. *Inorg. Chem.* **1995**, *35*, 643.

(51) Tatsumi, K.; Hoffmann, R. *Inorg. Chem.* **1980**, *19*, 2656.

(52) Dirand, J.; Ricard, L.; Weiss, R. *J. Chem. Soc., Dalton Trans.* **1976**, 278.

(53) Schlemper, E. O.; Schrauzer, G. N.; Hughes, L. A. *Polyhedron* **1984**, *3*, 377.

(54) Bristow, S.; Enemark, J. H.; Garner, C. D.; Minelli, M.; Morris, G. A.; Ortega, R. B. *Inorg. Chem.* **1985**, *24*, 4070.

(55) Cotton, F. A.; Wing, R. M. *Inorg. Chem.* **1965**, *4*, 867.

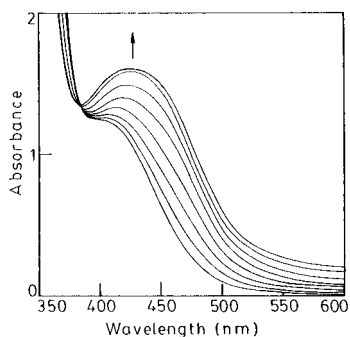


**Figure 3.** Spectral changes in the reaction of [MoO<sub>2</sub>L·CH<sub>3</sub>OH], **1** ( $4.0 \times 10^{-4}$  M), with H<sub>2</sub>tga ( $2.8 \times 10^{-2}$  M) in methanol at 10 °C. Spectra were recorded every 2 min over a period of 14 min.

ment reaction. The equatorial plane of this molecule and that of the phenyl ring of the ONPh group are not coplanar, as indicated by the Mo–O(4)–N(3)–C(11) torsion angle of 110.8°.

**Electronic Spectra.** The electronic spectra of **1** and **2** in methanol are relatively simple, each featuring a single ligand-to-metal  $S(\pi) \rightarrow Mo(d\pi)$  charge transfer band in the near-UV region at 405 (3070) and 402 nm ( $3000 \text{ M}^{-1} \text{ cm}^{-1}$ ), respectively. The corresponding band for the oxaziridine molecule **3** appears as a shoulder at 433 nm. For the Mo(IV) compound **4**, the spectrum recorded in degassed DMF appears to be a little more complicated by the presence of multiple absorptions.<sup>7d,19,56</sup> Following the ligand-field classification, it would be reasonable to assign the low-energy shoulder at 680 nm to a d–d transition ( $\epsilon 138 \text{ M}^{-1} \text{ cm}^{-1}$ ), while the remaining two high-intensity bands at 471 nm ( $5600 \text{ M}^{-1} \text{ cm}^{-1}$ ) and 402 nm (sh) are probably due to metal–ligand charge transfers. All the reported complexes have two UV bands appearing near or below 360 nm due to ligand internal transitions.

**Kinetics Studies: Oxygen Atom Transfer from [MoO<sub>2</sub>L·CH<sub>3</sub>OH].** The kinetics of reaction 5 were investigated in dry methanol under pseudo-first-order conditions by conventional spectrophotometry. At 25 °C, the reaction was followed to *ca.* 3 half-lives. The absorption band at 405 nm in **1** decays with time at the expense of a new band at 452 nm. The same reaction, when followed at 10 °C up to 1 half-life, generates a tight isobestic point at 382 nm with the peak position at 425 nm (Figure 3), consistent with the involvement of only two components under these conditions (*vide infra*). Pseudo-first-order plots of  $\log(A_\infty - A_t)$  against time (the symbols have their usual significance) indicate biphasic kinetics and are reminiscent of what is expected for a consecutive reaction scheme.<sup>57</sup> As shown in Figure 4, these plots can be resolved into two straight lines according to the method of Weyh and Hamm.<sup>58</sup> The straight-line segment corresponding to the longer time span when extrapolated to zero time, gives an intercept ( $A_e$ ) that accounts for the contribution of the second step relative to the earlier one. The observed rate constant for the second-step reaction ( $k_{\text{obs}}^{\text{II}}$ ) is obtained from the slope of the extrapolated line, and that of the first step ( $k_{\text{obs}}^{\text{I}}$ ) is determined by least-squares analysis of the line obtained from the logarithmic variation of corrected absorbances  $[(A_\infty - A_t) - A_e]$  versus time (Figure 4, inset).

These observed rates ( $k_{\text{obs}}^{\text{I}}$  and  $k_{\text{obs}}^{\text{II}}$ ) have first-order dependence on substrate concentration [H<sub>2</sub>tga] when present in large excess (Figure 5; see also Supporting Information). Equations

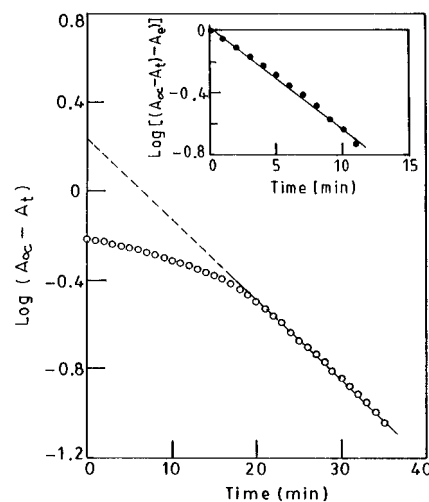


**Figure 4.** Kinetics plot for the reaction of [MoO<sub>2</sub>L·CH<sub>3</sub>OH] ( $4.22 \times 10^{-4}$  M) with H<sub>2</sub>tga ( $1.95 \times 10^{-2}$  M) at 10 °C, illustrating the biphasic nature of the reaction. Consecutive observed rate constants  $k_{\text{obs}}^{\text{I}}$  (inset) and  $k_{\text{obs}}^{\text{II}}$  were obtained from the slopes.

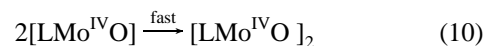
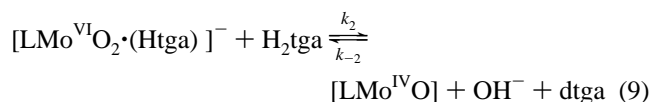
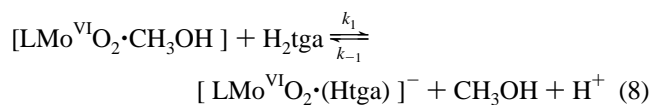
6 and 7 give the rate law dependencies for the two stages, where

$$k_{\text{obs}}^{\text{I}} = k_1[\text{H}_2\text{tga}] + k_{-1} \quad (6)$$

$$k_{\text{obs}}^{\text{II}} = k_2[\text{H}_2\text{tga}] + k_{-2} \quad (7)$$

$k_1$ ,  $k_2$  are the rates of forward reactions and  $k_{-1}$ ,  $k_{-2}$ , their backward contributions. The rate constants are calculated from the slopes and intercepts of the lines shown in Figure 5:  $k_1 = (72.08 \pm 4.98) \times 10^{-3} \text{ M}^{-1} \text{ s}^{-1}$ ,  $k_2 = (39.00 \pm 3.60) \times 10^{-3} \text{ M}^{-1} \text{ s}^{-1}$ ,  $k_{-1} = (1.11 \pm 0.09) \times 10^{-3} \text{ s}^{-1}$ , and  $k_{-2} = (0.56 \pm 0.07) \times 10^{-3} \text{ s}^{-1}$  at 10 °C. Corresponding values at 25 °C are  $(218.36 \pm 8.94) \times 10^{-3} \text{ M}^{-1} \text{ s}^{-1}$ ,  $(129.84 \pm 6.94) \times 10^{-3} \text{ M}^{-1} \text{ s}^{-1}$ ,  $(2.76 \pm 0.15) \times 10^{-3} \text{ s}^{-1}$ , and  $(1.75 \pm 0.11) \times 10^{-3} \text{ s}^{-1}$ , respectively. The observed values at 25 °C are approximately 3 times higher than those at 10 °C.

The overall reaction thus proceeds in two consecutive steps. Equations 8–10 provide a consistent interpretation. The first step is a substitution reaction involving replacement of the



coordinated methanol by a thioglycolate anion to generate a dioxomolybdenum(VI) species  $[\text{LMO}^{\text{VI}}\text{O}_2 \cdot (\text{Htga})]^-$  with sulfur from Htga<sup>-</sup> being the likely donor atom. The onset of this replacement process is clearly observable (Figure 3) in the form of an isobestic point at 10 °C up to *ca.* 1 half-life of the reaction beyond which the second step of the consecutive process becomes operative.

In the next step (eq 9), a second H<sub>2</sub>tga molecule generates the Mo(IV) product [LMO<sup>IV</sup>O] by an oxo-transfer reaction coupled to proton-electron transfers. The one-step two-electron Mo(VI)/Mo(IV) reduction is balanced electronically by the oxidation of 2 equiv of thiol to form the disulfide product (dtga). This crucial oxo-transfer step is particularly operative at 25 °C

(56) Laughlin, L. J.; Young, C. G. *Inorg. Chem.* **1996**, *35*, 1050.

(57) Wilkins, R. G. *Kinetics and Mechanism of Reactions of Transition Metal Complexes*, 2nd ed.; VCH: New York, 1991.

(58) Weyh, J. A.; Hamm, R. E. *Inorg. Chem.* **1969**, *8*, 2298.

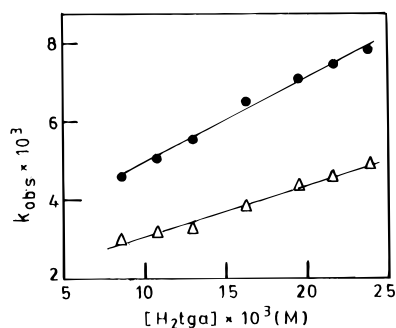


**Figure 5.** Dependence of observed rate constants  $k_{\text{obs}}^{\text{I}}$  (●) and  $k_{\text{obs}}^{\text{II}}$  (Δ) on  $[\text{H}_2\text{tga}]$  at 25 °C.

or higher temperature. At 10 °C, however, it occurs after the first half-life of the reaction, as previously mentioned. Finally, the monomeric Mo(IV) product is rapidly converted to a stable condensed form, perhaps binuclear (eq 10).

Oxo-transfer from *cis*-dioxomolybdenum(VI) compounds of sulfur ligands to oxomolybdenum(IV) products by arenethiols is known.<sup>49,59</sup> Comparatively less acidic aliphatic thiols, on the other hand, are capable of such reduction only in the presence of extraneous protons,<sup>60</sup> which presumably promote the rate of the oxo-transfer process through protonation of a terminal oxo ligand. Although  $\text{H}_2\text{tga}$  contains a much less acidic ( $\text{p}K_2 = 9.78$ ) aliphatic thiol group, it is the relatively stronger carboxylic acid component ( $\text{p}K_1 = 3.58$ )<sup>61</sup> that seems to serve as the source of protons needed to increase the electrophilicity of the molybdenum center, thus boosting the reduction process.

Martin and Spence<sup>34</sup> studied the oxidation of  $\text{H}_2\text{tga}$  by the Mo(VI) ion in aqueous media in a restricted pH range and found the reaction to proceed in two steps. Mo(VI) is reduced first to a  $\mu$ -oxo dimeric Mo(V)–tga complex and then to a stable Mo(IV) product of unknown composition. Under the present set of experimental conditions, the reaction of **1** with  $\text{H}_2\text{tga}$  appears to proceed through a Mo(VI) intermediate to an oxomolybdenum(IV) product. It is now accepted, almost as a general feature, that oxo-transfer reactions such as (1) are accompanied by the formation of a  $\mu$ -oxo Mo(V) dimer, either in an irreversible reaction or in an equilibrium process unless impeded by steric or geometrical restraints.<sup>6,62</sup> In the absence of a ligand with sufficient steric bulk, our present system presents an interesting example involving a Mo(IV) product

which is reluctant to undergo a comproportionation reaction with available Mo(VI) starting material. In fact, we have been successful in isolating the oxomolybdenum(IV) compound **4** from the *cis*-dioxo Mo(VI) precursor **1** by oxo abstraction in the presence of either  $\text{H}_2\text{tga}$  or  $\text{PPh}_3$ . In addition to its characteristic electronic spectral properties,<sup>6a,19</sup> **4** in an anaerobic medium is extremely inert to addition or substitution type reactions, which suggests a ligand-bridged structure (*vide supra*) for this compound with sufficient geometrical constraints to form a  $\mu$ -oxo Mo(V) dimer. Bhattacharyya et al. in a recent report<sup>36</sup> identified **4** as a Mo(IV) compound with a polymeric structure. Holm et al.,<sup>6a</sup> following the structure determination of an analogous zinc(II) complex,<sup>63</sup> proposed a similar thiolato-bridged dimeric structure as a viable alternative for the molybdenum(IV) complex  $[\text{MoO}(\text{L-NS}_2)(\text{DMF})]$  ( $\text{L-NS}_2 = 2,6$ -bis(2,2-diphenyl-2-sulfidoethyl)pyridinate(2-)), which is known to hinder  $\mu$ -oxo Mo(V) dimer formation.<sup>25</sup>

### Concluding Remarks

Two substrates PhNHOH and  $\text{H}_2\text{tga}$ , both known to function simultaneously as proton and electron donors,<sup>34,35</sup> have been used to study the reactivity pattern of Mo–O<sub>t</sub> bonds associated with an anionic sulfur ligand. With PhNHOH, the product of the reaction with **1** is a seven-coordinate oxaziridine Mo(VI) compound **3**, formed by the rearrangement of one terminal oxo ligand. The Mo–O<sub>t</sub> distance involving the remaining (spectator) oxo ligand O(1) in **3** is drastically reduced to 1.668(2) Å, typical of Mo–O bonds of order 3, and can be explained as being due to the one  $\sigma$  and two  $\pi$  bonds which the spectator oxo ligand is allowed to form on removal of the other oxygen atom from the *cis*-MoO<sub>2</sub> moiety.<sup>55,64</sup> This observation is a classic example of spectator oxo stabilization of a strained metallacycle as predicted by Rappé and Goddard.<sup>48</sup> With  $\text{H}_2\text{tga}$ , on the other hand, an oxygen atom transfer reaction proceeds through coupled electron–proton transfer steps that successfully model the turnover reaction of oxidoreductase Mo enzymes.

**Acknowledgment.** We wish to thank Professor P. Banerjee for helpful discussions. Financial assistance received from the Council of Scientific and Industrial Research, New Delhi, is gratefully acknowledged.

**Supporting Information Available:** Tables of atomic coordinates, anisotropic thermal parameters, bond distances and angles, least-squares planes, torsional angles, and kinetics data ( $k_{\text{obs}}$  vs  $[\text{H}_2\text{tga}]$ ) (17 pages). Ordering information is given on any current masthead page. Structure factor amplitudes are available from the authors on request.

IC960670Z

(59) McDonald, J. W.; Corbin, J. L.; Newton, W. E. *Inorg. Chem.* **1976**, *15*, 2056.

(60) Llopis, E.; Domenech, A.; Ramirez, T. A.; Cervilla, A.; Palanca, P.; Picher, T.; Sanz, V. *Inorg. Chim. Acta* **1991**, *189*, 29.

(61) *Stability Constants of Metal Ion Complexes*; Sillen, L. G., Martell, A. E., Eds.; Special Publication No. 17; The Chemical Society: London, 1964; p 376.

(62) (a) Subramanian, P.; Spence, J. T.; Ortega, R.; Enemark, J. H. *Inorg. Chem.* **1984**, *23*, 2564. (b) Spence, J. T.; Minelli, M.; Kroneck, P. *J. Am. Chem. Soc.* **1980**, *102*, 4538.

(63) Kaptein, B.; Wang-Griffin, L.; Barf, G.; Kellogg, R. M. *J. Chem. Soc., Chem. Commun.* **1987**, 1457.

(64) Schröder, F. A. *Acta Crystallogr.* **1975**, *B31*, 2294.